

Creep of a fracture line in paper peeling

J. Koivisto, J. Rosti, and M.J. Alava
*Helsinki University of Technology, Laboratory of Physics,
 P.O.Box 1100, FIN-02015 HUT, Finland*

The slow motion of a crack line is studied via an experiment in which sheets of paper are split into two halves in a “peel-in-nip” (PIN) geometry under a constant load, in creep. The velocity-force relation is exponential. The dynamics of the fracture line exhibits intermittency, or avalanches, which are studied using acoustic emission. The energy statistics is a power-law, with the exponent $\beta \sim 1.8 \pm 0.1$. Both the waiting times between subsequent events and the displacement of the fracture line imply complicated stick-slip dynamics. We discuss the correspondence to tensile PIN tests and other similar experiments on in-plane fracture and the theory of creep for elastic manifolds.

PACS numbers: 62.20.Mk, 05.70.Ln, 81.40.Lm, 62.20.Fe

The deformation and fracture of materials is a fascinating topic as one can explore the physics even without sophisticated experiments [1]. A piece of paper suffices to give ample evidence for the presence of phenomena that need a statistical description. One can tear a sheet or crumble it, to observe that the response is “intermittent” and not simply “smooth”. [2, 3, 4, 5].

The physics of fracture in a material as paper is governed by two basic ingredients. The structure and the microscopic material properties are inhomogeneous, while the stress fields follow the laws of elasticity. Typical statistical signatures that show features that emerge from their interaction are the acoustic emission during a deformation test and the post-failure properties of fracture surfaces. These are commonly found to be described by power-laws, as regards the energies of acoustic events (“earthquakes”), the intervals between subsequent events (“Omori’s law”) [4, 6], and the same is true for the geometry of cracks where ample evidence points towards a self-affine fractal scaling of the surface fluctuations around the mean, which is found in a variety of cases (loading conditions, materials and so forth) [7, 8, 9].

The most simple case of fracture - which we also will study here - is the passage of a *crack line* through a sample, when its movement is constrained on a plane. In this case, the mathematical description is given by a crack position $h(x, t)$, where x is along the average projection of the crack. The average motion is described by $\dot{h} = vt$ with v the crack velocity. In the situation at hand one has three ingredients: a disordered environment which poses obstacles to the line motion, a driving force K_{ext} (stress intensity factor in fracture mechanics language), and the self-coupling of the fluctuations in h through a long-range elastic kernel [10], which is expected to scale as $1/x$.

To describe the line’s physics one needs the language of statistical mechanics. One finds a phase diagram for $v(K_{ext})$: an immobile crack begins to move at a critical value K_c of K_{eff} such that for $K > K_c$ $v > 0$. This transition between a “mobile line” and a pinned line is commonly called in non-equilibrium statistical mechan-

ics a “depinning transition”. Close to the critical point K_c the line geometry is a self-affine fractal with a roughness exponent ζ . This is an example of a wide class of similar problems, which range from fire fronts in combustion to flow fronts in porous media to domain walls in magnets. The planar crack [11] or the contact line on a substrate [12] problem has been studied both theoretically via renormalization group calculations and numerical simulations, and via experiments. There is a discrepancy between these, in that the roughness exponents are $\zeta_{theory} \sim 0.39$ and $\zeta_{expt} \sim 0.6$ [13, 14]. In three-dimensional experiments the in-plane roughness has recently shown signatures of $\zeta_{expt} \sim \zeta_{theory}$ [15]. Imaging experiments have shown the existence of *avalanches*, of localized intermittent advances of the crack front with an avalanche size s distribution $P(s) \sim s^{-1.6 \dots -1.7}$ [13]

Our work considers the dynamics of such a crack front during *creep*, which is done by peeling paper sheets in a geometry illustrated in Fig. 1 (see also [16]). The creep of elastic lines (or manifolds or domain walls) is important since when $K_{eff} \leq K_c$ thermal fluctuations take over for $T > 0$ [17, 18, 19]. The fluctuations nucleate “avalanches” similarly to what happens in zero-temperature depinning in the vicinity of K_c . The avalanches induce a finite velocity v_{creep} . The advancement of a crack front might be fundamentally different from say a domain wall or a contact line, which can fluctuate back and forth around a metastable state: it is easy to see that the crack may in many cases only grow forward.

The form of $v_{creep}(K_{eff}, T)$ depends on the “energy landscape” since the current understanding is that creep takes place via nucleation events over energy barriers [17]. These barriers are related to the roughness exponent ζ and to its origins. The important physics is summarized with the creep formula

$$v_{creep} \sim \exp(-C/m^\mu) \quad (1)$$

which states that the creep velocity is related to the driving force, m (as for mass, see Fig. 1 again),. There is a *creep exponent* μ , which depends on the interactions and

dimension of the moving object (a line). One expects the scaling

$$\mu = \theta/\nu = \frac{\alpha - 2 + 2\zeta}{\alpha - \zeta} \quad (2)$$

in d dimensions. ($d = 1$ for a line, $d = 2$ for a domain wall in say a bulk magnet). θ , ν , and ζ denote the energy fluctuation, correlation length, and roughness exponents relevant for the problem, and exponent relations are usually postulated between these three. They exponents all depend on α , the k -space decay exponent of the elastic kernel. For long range elasticity, one would assume $\alpha = 1$ whereas for the so-called local case $\alpha = 2$ is expected. Expressed as above, the question of the value of μ boils down to the values of ζ and α - what is the effective roughness at hand, and what is the elasticity of the line like?

The fundamental formula of Eq. (2) has been confirmed in the particular case of 1+1-dimensional domain walls [20], and further experimental studies exist [21]. Our main results on fracture line creep concern the velocity-force-relation $v(m)$, and on the picture of the dynamics that ensues, in particular from Acoustic Emission (AE) data of the avalanches and their dynamics. We find an exponential $v(m)$ and discuss its interpretations. The dynamics shows signatures of intriguing but weak correlations, and we discuss the similarities and differences to the tensile case.

In Figure 1 we show the apparatus [22]. The failure line can be located along ridge, in center of the the Y-shaped construction formed by the unpeeled part of the sheet (below) and the two parts separated by the advancing line. Diagnostics consist of an Omron Z4D-F04 laser distance sensor for the displacement, and a standard plate-like piezoelectric sensor [22]. It is attached to the setup inside one of the rolls visible in Fig. 1, and the signal is filtered and amplified using standard techniques. The data acquisition card has four channels at 312.5 kHz per channel. We finally threshold the AE data. The displacement data is as expected highly correlated with the corresponding AE, but the latter turns out to be much less noise-free and thus convenient to study. For paper, we use perfectly standard copy paper, with an areal mass or basis weight of 80 g/m². Industrial paper has two principal directions, called the ‘‘Cross’’ and ‘‘Machine’’ Directions (MD/CD) [23]. The deformation characteristics are much more ductile in CD than in MD, but the fracture stress is higher in MD. We tested a number of samples for both directions, with strips of width 30 mm. The weight used for the creep ranges from 380 g (CD) to 533 g (MD), and the resulting data has upto to tens of thousands of AE events (avalanches) per test (Fig. 3). It is unfortunately not possible to infer the critical depinning $m_c > m_{used}$. The mechanical (and creep) properties of paper depend on the temperature and humidity. In our setup both remain at constant levels during an experi-

ment, and the typical pair of values for the environment is 49 rH and 27 °C (though we also have data for other combinations).

Our main result is given in Figure 4, where we show the $v(m)$ vs. $1/m$ characteristics. There are four main datasets depicted. These differ slightly in the typical temperature and humidity (for set 2 44 % rH instead of about 49 % rH for the others). These all imply an *exponential* behavior, and by fits to the data sets we can infer a creep exponent $\nu = 1.0 \pm 0.1$. This lends itself to two different interpretations: either the creep is in the 1d random field (RF) domain wall universality class, since with $\alpha = 2$ $\nu = 1$ implies $\zeta = 1$, the roughness exponent of the RF universality class at very small external fields/forces. This assumes *local elasticity* being dominant. If we would then assume that ζ takes the value $\zeta \sim 0.6 \dots 0.7$, of the avalanche regime, this would imply screened interactions with $\alpha \sim 1.4$. The third possibility is to use non-local line elasticity, with $\alpha = 1$. Then Eq. 2 indicates that $\zeta \sim 1/3$. This is exactly the *equilibrium* exponent of lines with long-range elasticity [26]. The velocity in the case of ‘‘paper’’ is influenced by the humidity: this is clear in our case. Meanwhile, note that the temperature variation is insignificant here.

The avalanche behavior is illustrated by Fig. 4a, by the way of the AE event energy distribution $P(E)$. We present two kinds of avalanche data: integrated over 1 ms windows (E_i where i is an integer time index for CD) and extracted from single avalanches. The former obviously sums over all the avalanches during the 1 ms duration (if more than one are present). The data agrees rather well regardless of the mass m and the ductility (CD, MD) with the scaling $P(E) \sim E^{-\beta}$ with $\beta = 1.7 \pm 0.1$. This β is close to the one observed in the corresponding tensile experiment (depicted in the Fig. 4a) [22]. The simplest interpretation would be that once an avalanche is created through a thermal fluctuation, it follows a deterministic course. This is similar to the predictions of recent theories, which indicate the presence of a small nucleation scale, and that the avalanches should be as at the depinning critical point [18, 19, 24].

We have studied the temporal statistics and correlations using the AE timeseries, in particular the windowed one, and the direct displacement vs. time -signal (note that the AE has better accuracy in the time domain). The waiting times τ , the silent intervals between either two avalanches or two windows with $E_i > 0$ are shown in Fig. 4b. It is interesting to note how the distributions $P(\tau) \sim \tau^\alpha$ change with the applied force. For large driving forces it appears that there are (perhaps) two power-law like regimes: one with an exponent $\alpha = 1.3$, and more clearly one for large τ with $\alpha \sim 2$ which is also found for m small. The general form for m large resembles also that of similar tensile tests where $\alpha \sim 1$ is found. In the tensile case, there is a typical time/lengthscale (arising from paper structure) visible in tensile crackline tests,

which might here also be related to the change in the slope of $P(\tau)$.

The dynamics of the line exhibits stick-slip: the integrated velocity depends on the window length under consideration. This is already evident from the $P(E)$ and extends to longer timescales than what $P(E)$ implies via durations of events. A “stick-slip” exponent can be extracted also from the displacement data as well as integrated from the AE data. It appears that a relation $P(\Delta h) \sim \Delta h^{-1.7}$ arises. This implies the presence of correlations, which we next study by the energy release rate T : the duration of the active time T as measured as subsequent windows where $E_i > 0$. It can be seen as illustrated in Figure 5 that $P(T) \sim T^{-2.7}$, so that on a millisecond scale (much slower than avalanche durations, but much faster than the inverse line velocity) there are clear correlations. These are however *weak* in the respect that one can not see in here or the AE data signatures of “aftershocks” or “precursors” familiar from earthquakes or from the AE activity of dislocation systems [25]. One may also see a correlation between the energy released in the active period vs. its duration, such that $E_{tot} \sim T^{0.25}$ at least for m small. Thus it appears that the temporal dynamics can be described by a temporal self-affine process.

To conclude, we have studied the creep dynamics of an elastic line, or a fracture front in peeling paper sheets. The particular features of our case are the disorder present in usual paper and the variation in material properties (ductile/brittle). The main findings are four-fold. First, we have obtained an exponential velocity-force relation, which has three interpretations; we prefer the one which assumes non-local elasticity implying that an equilibrium $\zeta \sim 1/3$ governs the creep. Second, we observe intriguing similarities and differences in AE or avalanches to ordinary tensile (constant, small velocity) experiments. These, third, indicate the separation of deterministic, zero-temperature dynamics from the nucleation - as in creep indeed - of individual events. Fourth, the dynamics of the process exhibits correlations that would need a theoretical explanation. Our results clearly call for more theoretical effort to understand in-plane fracture fronts, and their creep properties. They also indicate the need for general studies of creep fracture as a statistical physics problem. **Acknowledgments:** The Center of Excellence program of the Academy of Finland is thanked for financial support as well as KCL Ltd and the funding of TEKES, Finnish Funding Agency for Technology and Innovation. R. Wathén, J. Lohi, and K. Niskanen contributed both with moral and practical support. L. Ponson is acknowledged for a crucial reminder.

- [2] J.P. Sethna, K.A. Dahmen, and C.R. Myers, Nature (London) **410**, 242 (2001), one can also “crumble” and listen; P.A. Houle and J.P. Sethna, Phys. Rev. **E54**, 278 (1996).
- [3] J. Kertész, V. K. Horvath, and F. Weber, Fractals **1**, 67 (1993).
- [4] L.I. Salminen, A.I. Tolvanen, and M.J. Alava, Phys. Rev. Lett. **89**, 185503 (2002).
- [5] S. Santucci, L. Vanel, and S. Ciliberto Phys. Rev. Lett. **93**, 095505 (2004).
- [6] A. Guarino, A. Garcimartin, and S. Ciliberto, Eur. Phys. J. B **6**, 13 (1998); A. Garcimartin, A. Guarino, L. Bellon, and S. Ciliberto, Phys. Rev. Lett **79**, 3202 (1997).
- [7] B. B. Mandelbrot, D. E. Passoja, and A. J. Paullay, Nature (London) **308**, 721 (1984).
- [8] E. Bouchaud, J. Phys. Cond. Mat. **9**, 4319 (1997).
- [9] L. Ponson, D. Bonamy, and E. Bouchaud, Phys. Rev. Lett. **96**, 035506 (2006).
- [10] D. Fisher, Phys. Rep. **301**, 113 (1998).
- [11] S. Ramanathan and D.S. Fisher, Phys. Rev. Lett. **79**, 877 (1997).
- [12] J. F. Joanny, P. G. De Gennes, J. Chem. Phys., **81**, 552 (1984); S. Moulinet, C. Guthmann, E. Rolley, Eur. Phys. J. E, **8**, 437 (2002); A. Prevost, E. Rolley, C. Guthmann, Phys. Rev. B, **65**, 064517 (2002); P. Le Doussal, K.J. Wiese, E. Raphael, and R. Golestanian, Phys. Rev. Lett. **96**, 015702 (2005).
- [13] J. Schmittbuhl and K.J. Mløy, Phys. Rev. Lett. **78**, 3888 (1997); K.J. Mløy et al., Phys. Rev. Lett. **96**, 045501 (2006),
- [14] A. Rosso and W. Krauth, Phys. Rev. Lett. **87**, 187002 (2001); O. Dummer and W. Krauth, cond-mat/0612323.
- [15] D. Bonamy, L. Ponson, S. Prades, E. Bouchaud, and C. Guillot, Phys. Rev. Lett. **97**, 135504 (2006).
- [16] Rumi De and G. Ananthakrishna Phys. Rev. Lett. **97**, 165503 (2006)
- [17] T. Nattermann, Europhys. Lett. **4**, 1241 (1987); L.B. Ioffe and V.M. Vinokur, J. Phys. C **20**, 6149 (1987); T. Nattermann, Y. Shapir, and I. Vilfan, Phys. Rev. B **42**, 8577 (1990).
- [18] P. Chauve, T. Giamarchi, and P. Le Doussal, Phys. Rev. **E62**, 6241 (2000).
- [19] A. B. Kolton, A. Rosso, and T. Giamarchi, Phys. Rev. Lett. **94**, 047002 (2005).
- [20] S. Lemerle et al., Phys. Rev. Lett. **80**, 849 (1998)
- [21] Th. Braun, W. Kleemann, J. Dec, and P. A. Thomas, Phys. Rev. Lett. **94**, 117601 (2005); T. Tybell, P. Paruch, T. Giamarchi, and J.-M. Triscone, Phys. Rev. Lett. **89**, 097601 (2002).
- [22] L.I. Salminen et al., Europhys. Lett. **73**, 55 (2006).
- [23] M.J. Alava and K.J. Niskanen, Rep. Prog. Phys. **69**, 669 (2006).
- [24] A.B. Kolton, A. Rosso, T. Giamarchi, and W. Krauth Phys. Rev. Lett. **94**, 057001 (2006)
- [25] J. Weiss and D. Marsan, Science **299**, 89 (2003).
- [26] P. Le Doussal, K.J. Wiese, and P. Chauve, Phys. Rev. **E69**, 026112 (2004).

[1] M.J. Alava, P.N.N.K. Nukala, and S. Zapperi, Adv. Phys. **54**, 347 (2006).

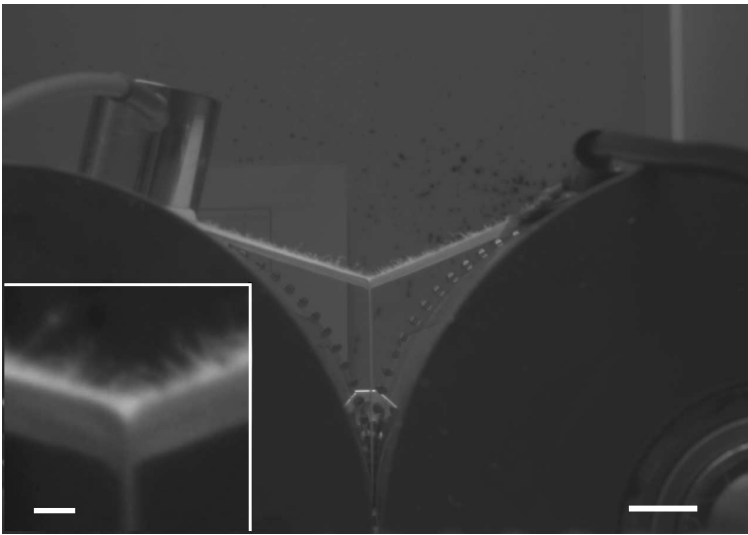
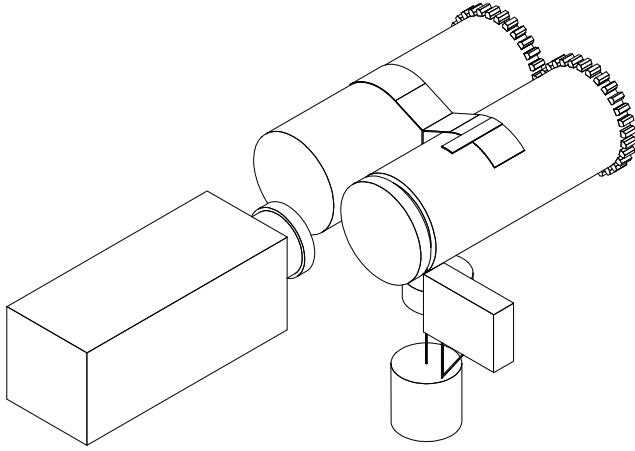


FIG. 1: Schematic view of the experimental setup (rolls, paper, AE sensor, camera, weight), and two closer views of the geometry.

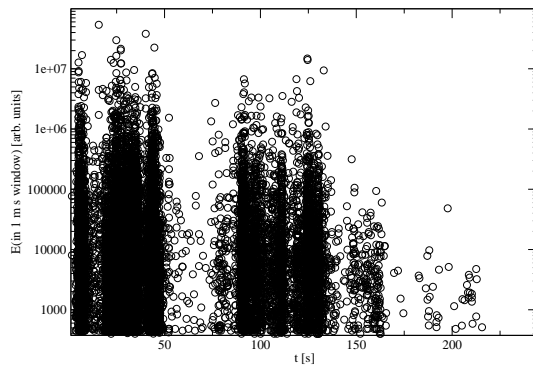


FIG. 2: An example of the acoustic or stick-slip activity ($E_i > 0$) during one single creep test. The energy E_i is integrated after thresholding over 1 ms windows.

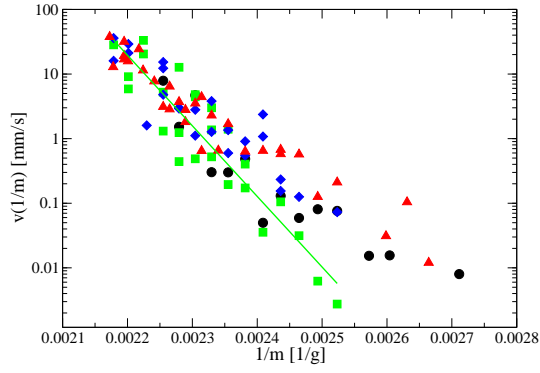


FIG. 3: The creep velocity vs. the inverse of the applied force or mass. The line indicates an exponential decay ($v \sim \exp a/m$). The four sets (circle, rectangle, diamond, triangle) differ such that the 2nd one was done under lower relative humidity, rH % 43).

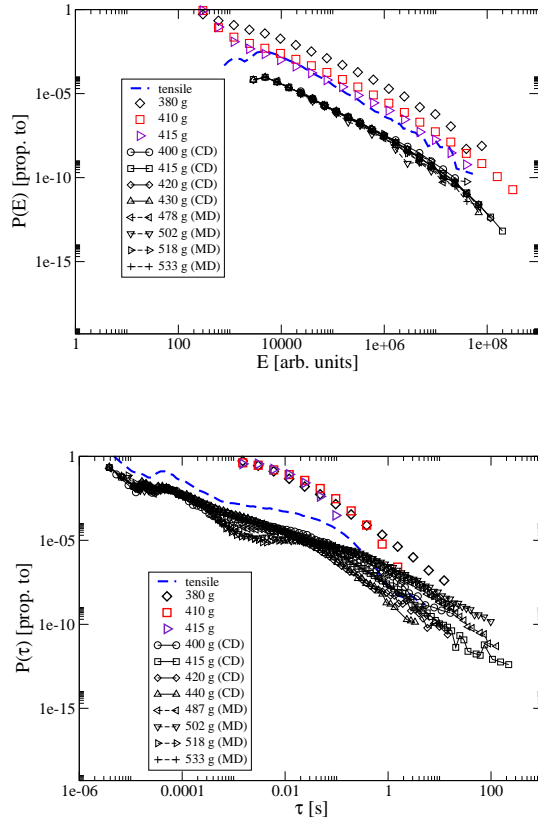


FIG. 4: a): The probability distributions of the acoustic events for various cases. b): pots of the event interval (waiting time) distributions, for different masses m . The data sets have been shifted for clarity.

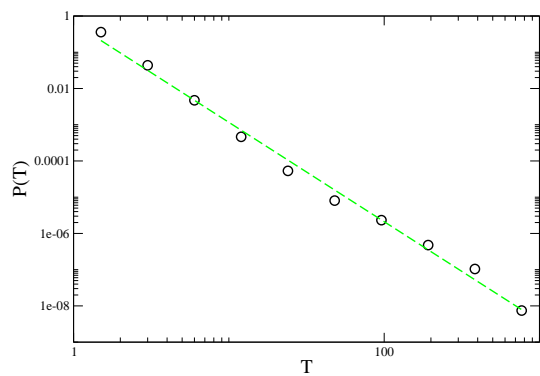


FIG. 5: The $P(T)$ of durations of active times T (for definition of T see text) The line has slope -2.7.